PASJ: Publ. Astron. Soc. Japan **64**, 44, 2012 June 25

OAO/ISLE Near-IR Spectroscopy of IRAS Galaxies

Yoshiki MATSUOKA, Fang-Ting YUAN, and Yoshitaka TAKEUCHI
Graduate School of Science, Nagoya University, Furo-cho, Chikusa-ku, Nagoya 464-8602
matsuoka@a.phys.nagoya-u.ac.jp
and
Kenshi YANAGISAWA
Okayama Astrophysical Observatory, National Astronomical Observatory of Japan, Kamogata, Asaguchi, Okayama 719-0232

(Received 2011 July 16; accepted 2011 November 10)

Abstract

We present the results of the near-infrared (IR) spectroscopy of nine IRAS galaxies (NGC 1266, NGC 1320, NGC 2633, NGC 2903, NGC 3034, Mrk 33, NGC 7331, NGC 7625, NGC 7714) with the ISLE imager and spectrograph mounted on the Okayama Astrophysical Observatory 1.88-m telescope. [Fe II] 1.257 μm and Paβ emission lines were observed for the whole sample, while H_2 2.121 μm and Brγ lines were additionally obtained for two sources, whose flux ratios were used as a diagnostic tool of dominant energy sources of the galaxies. We found that the nucleus of NGC 1266 is most likely a low-ionization nuclear emission-line region (LINER), while NGC 2633 and NGC 2903 possibly harbor active galactic nuclei (AGNs). No AGN or LINER signal is found for other objects. In addition, we found the spectral features, which are indicative of some unusual phenomena occurring in the galaxies, such as the large [Fe II] line widths compared to the local escape velocity in NGC 1266. The present work shows the potential ability of ISLE to shed new light on the nature of infrared galaxies, either through a statistical survey of galaxies or an exploration of spectral features found in individual objects.

Key words: galaxies: active — galaxies: evolution — galaxies: individual (NGC 1266, NGC 1320, NGC 2633, NGC 2903, NGC 3034, Mrk 33, NGC 7331, NGC 7625, NGC 7714) — infrared: galaxies

1. Introduction

One of the major achievements of the Infrared Astronomical Satellite (IRAS) is the discovery of a significant number of galaxies emitting the bulk of their radiation at far-infrared (IR) wavelengths. Luminous IR galaxies (LIRGs: with IR luminosity $L_{\rm IR} > 10^{11}\,L_\odot$) are as numerous as optical starburst and Seyfert galaxies with similar bolometric luminosity in the local universe, while the more extreme class of ultra-luminous IR galaxies (ULIRGs: $L_{\rm IR} > 10^{12}\,L_\odot$) has a similar space density and bolometric luminosity to optically-selected quasars (Soifer et al. 1987). Many studies have been devoted to exploring the origin of these IR galaxies, and it is now becoming a general agreement that strong interactions and mergers of gas-rich galaxies are the trigger for the majority of them. In the complete sample of IRAS 1 Jy ULIRGs, Veilleux, Kim, and Sanders (2002) found that nearly 100% of the IR galaxies show strong signs of tidal interactions.

On the other hand, there is still much debate about the energy sources of IR galaxies. Their IR luminosity can certainly come from dust reprocessing of radiations from starburst and/or active galactic nuclei (AGNs) activity. In this context, it is worth noting that ULIRGs and AGNs most probably have evolutionary connection. It is suggested that the major mergers of gas-rich galaxies first form a "cool" ULIRG dominated by dusty starburst, which is followed by a "warm" ULIRG phase when an AGN turns on and starts to heat the surrounding dust. Then, the AGN evolves into the dominant energy source, and blows away the surrounding dust cocoon, leading to an optically-bright quasar (e.g., Lonsdale et al. 2006). Therefore, an observational probe of the energy sources in IR galaxies at various evolutionary stages is a key for understanding the whole picture of galaxy evolution, including the AGN phase. However, such studies have been hampered by heavy dust obscuration inside IR galaxies. Although numerous efforts have been devoted to the subject at various wavelengths (e.g., Veilleux et al. 1995; Tran et al. 2001; Ptak et al. 2003; Farrah et al. 2007; Imanishi et al. 2007), the results are still largely controversial; different studies give inconsistent estimates of the relative contributions from starburst and AGNs for the same population.

In order to address the issue of energy sources in IR galaxies, we aim to investigate the presence of AGNs independently from previous studies, in a large number of IR galaxies, including ULIRGs, LIRGs, and less-luminous populations. In this paper, we present the near-IR spectra of nine IRAS galaxies with relatively low IR luminosity, obtained by the ISLE imager and spectrograph mounted on the Okayama Astrophysical Observatory (OAO) 1.88-m telescope. Near-IR light has a few advantages over those at other wavelengths in probing IR galaxies. First, it suffers much less from dust obscuration than optical light, since the extinction at the former wavelengths is only about one tenth of that at the latter (i.e., $A_K \sim 0.1\,A_V$). Second, near-IR observations cost much less than X-ray, mid- or far-IR observations, and hence a statistical number of objects can be easily investigated. Third, there are many emission lines suitable for probing their radiation sources in the near-IR spectral region (e.g., Matsuoka et al. 2007, 2008). Veilleux, Sanders, and Kim (1999) demonstrated the power of near-IR spectroscopy by observing 39 ULIRGs, and finding that at least 50% of the optically-classified Seyfert 2 galaxies present hidden broad-line-region (BLR) emissions in near-IR lines. This means that the nuclear regions of many optical Seyfert 2 galaxies, completely obscured in optical wave bands, are optically thin at near-IR wave bands.

We observed four near-IR emission lines: [Fe II] 1.257 μm and Paβ for the whole sample of nine galaxies and H_2 2.121 μm and Brγ for two of them, whose flux ratios have been proposed as a diagnostic tool of dominant energy sources of emission-line galaxies (Larkin et al. 1998; Rodríguez-Ardila et al. 2005). Note that this kind of diagnostic diagrams work only with a statistical number of samples, since there are always outlying objects. In this sense, we do not intend to present conclusive arguments with the small number of objects observed in this work, but rather aim to demonstrate the capability of ISLE to investigate the near-IR emission lines of IR galaxies for future projects. Hereafter, [Fe II] 1.257 μm and H_2 2.121 μm lines are abbreviated as [Fe II] and H_2 for simplicity.

2. Observation and Data Reduction

The observation targets were selected from the Imperial IRAS-FSC Redshift Catalog (IIFSCz: Wang & Rowan-Robinson 2009) based on the IRAS Faint Source Catalog (FSC). The observability of the four emission lines ([Fe II], Paβ, H_2, and Brγ) in the near-IR atmospheric window gives a severe restriction on the redshifts, while the additional constraints come from the positions and near-IR brightness ($J < 12$ mag). We summarize the redshifts, the Two Micron All Sky Survey (2MASS: Skrutskie et al. 2006) J-band magnitudes, 60-μm fluxes ($f_{60\mu\mathrm{m}}$) and IR luminosity (L_{IR}) based on the IRAS measurements, and corresponding IRAS names of the targets in table 1. They are not extremely luminous at the IR wavelengths compared to LIRGs or ULIRGs.

The observation was carried out with the ISLE, a near-IR imager and spectrograph mounted on the OAO 1.88-m telescope (Yanagisawa et al. 2006, 2008). The instrument uses a HAWAII 1 k $\times$ 1 k array, which provides a 4.′3 $\times$ 4.′3 field-of-view with a pixel scale of 0.″25. The useful wavelength intervals covered by the J, H, and K filters are 1.11–1.32 μm, 1.50–1.79 μm, and 2.02–2.37 μm, respectively. The slit length and the orientation are fixed to 4′ and the east–west direction, respectively.

The observation journal is given in table 2. For each object, we first carried out a J-band observation, and then decided the priority of taking additional H- or K-band data based on the J-band spectrum. As a result, the H-band spectrum was taken for NGC 1266 and the K-band spectra were taken for NGC 2633 and NGC 2903 (more details are given in the following section). The sky condition was sometimes non-photometric during the nights. We used a 2.″0 slit, which provided wavelength resolutions of $R \sim 1200$, 1800, and 1000

Table 1. Targets summary.

Name	Redshift	J (mag)	$f_{60\mu\mathrm{m}}$ (Jy)	log L_{IR} ($L_{\odot}$)	IRAS name
NGC 1266	0.0073	10.66	12.83	10.44	F03135−0236
NGC 1320	0.0089	10.47	2.15	10.24	F03222−0313
NGC 2633	0.0072	10.13	15.87	10.65	F08425+7416
NGC 2903	0.0019	7.03	47.62	10.10	F09293+2143
NGC 3034	0.0007	5.88	1217.26	10.41	F09517+6954
Mrk 33	0.0048	11.61	4.68	9.71	F10293+5439
NGC 7331	0.0027	7.16	32.08	10.29	F22347+3409
NGC 7625	0.0054	9.98	9.33	10.25	F23179+1657
NGC 7714	0.0093	10.84	10.36	10.66	F23336+0152

Table 2. Observation journal.

Target	Date	Band	Exp time (min)	Standard stars
NGC 1266	2010 Dec 09	J	128	HD 13936, HD 32996
	2010 Dec 10	H	64	HD 13936, HD 32996
NGC 1320	2010 Dec 08	J	80	HD 31411
NGC 2633	2010 Dec 09	J	68	HD 55075
	2010 Dec 09	K	56	HD 55075, HD 71906
NGC 2903	2010 Dec 10	J	32	HD 55075, HD 89239
	2010 Dec 10	K	64	HD 89239
NGC 3034	2010 Dec 10	J	16	HD 55075, HD 89239
Mrk 33	2010 Dec 08	J	80	HD 92728
NGC 7331	2010 Dec 09	J	32	HD 211096, HD 13936
NGC 7625	2010 Dec 10	J	108	HD 208108, HD 1439
NGC 7714	2010 Dec 09	J	32	HD 208108, HD 211096

at the J, H, and K bands, respectively. The choice of the relatively wide slit was effective in reducing the amplitudes of the fringe patterns, which often dominate the measurement errors at the red part of the spectra. The total exposure times were broken into individual exposures of 120 s, and the objects were offset along the spatial direction of the slit between adjacent exposures. We observed A0 V–A0 III stars for flux calibration immediately before or after the target exposures at similar airmass.

Data reduction was performed in a standard manner. After dark subtraction and flat fielding, the sky emission was eliminated by subtracting an adjacent offset image. Then, the residual sky background was estimated from counts of nearby pixels in the spatial direction and removed. We extracted the target spectra within a 5."0 (20-pixel) aperture, whose size is close to the full width at zero intensity of the point spread function, in all but the J-band images of NGC 7331 and NGC 1266, requiring a larger 7."6 (30-pixel) aperture, due to poor seeing. The apertures were centered on the spatial peak positions of the spectra. All of the galaxies have apparent sizes of $> 10''$, and hence the resultant spectra were sampled from only their central regions. We also note that the estimated sky backgrounds could contain contributions from the outer galaxies. Such a contamination would reduce the galaxy contributions in the extracted spectra, which might result in a slight enhancement of the relative contribution of the AGNs. However, the signal-to-noise ratios of outer galaxy regions in our data are not high enough to quantify these contributions. Wavelength calibration was achieved by referring to the Ar arc spectra obtained with the same instrument configuration as used for the target observation. The mean RMS values of the calibration were 0.9, 3.4, and 1.7 Å in J, H, and K bands, respectively. The atmospheric and instrumental transmissions were estimated from the observed spectra of the A0 standard stars, for which we assumed an intrinsic black-body spectrum with an effective temperature of 9600 K (Pickles 1998) after the stellar H I recombination lines were manually removed.

3. Results and Discussion

We show the reduced spectra around the four emission lines, as well as [Fe II] 1.644 μm for NGC 1266, in figure 1. To the detected lines, we fit Gaussian functions with underlying continua represented by tilted lines, i.e.,

$$F(v) = a_0 \exp\left[-\frac{(v-a_1)^2}{2a_2^2}\right] + (a_3 + a_4 v), \qquad (1)$$

where v represents the velocity shift relative to the line centers. The free parameters (a_0, a_1, a_2, a_3, and a_4) were determined simultaneously by fitting the function to the observed spectra with the least-χ^2 method within the velocity range from -2000 to $+2000\,\mathrm{km\,s^{-1}}$. We show the fitted functions in figure 1. The equivalent widths (*EW*s) and the full widths at half maximum (*FWHM*s) of the emission lines derived from the best-fit parameters are summarized in table 3. The *FWHM*s were corrected for the instrumental resolution, assuming $R = 1200$, 1800, and 1000 in the J, H, and K bands, respectively. The upper limit of $300\,\mathrm{km\,s^{-1}}$ was given to the lines with the measured *FWHM*s less than the instrumental resolution. The reduced χ^2 values are close to unity in all cases. Note that we use *EW*s and flux ratios, rather than absolute flux values, since the latter is subject to unknown amounts of aperture loss.

The measured line-flux ratios of [Fe II]/Paβ and H_2/Brγ are plotted in figure 2. Larkin et al. (1998) suggested this diagram as a diagnostic tool for energy sources of the line emissions. Later, the classification scheme was updated by Rodríguez-Ardila et al. (2004) and Rodríguez-Ardila, Riffel, and Pastoriza (2005), who found that AGNs are characterized by the two ratios between 0.6 and 2, while the smaller or larger values indicate starburst/H II galaxies, or low-ionization nuclear emission-line regions (LINERs), respectively (dotted lines in figure 2). However, note that this diagnostic diagram works only with a statistical number of samples, since there are objects that do not meet the above criteria in the compilation of Rodríguez-Ardila, Riffel, and Pastoriza (2005).

The most noticeable object in figure 2 is NGC 1266. Its [Fe II] line flux is at least 10-times larger than Paβ, clearly indicating that it is a LINER. Therefore, we obtained an additional H-band spectrum, and found that another [Fe II] line, [Fe II] 1.644 μm, is also strong in this object. The *FWHM*s of the two [Fe II] lines, $\sim$500 $\mathrm{km\,s^{-1}}$, are significantly larger than the local escape velocity ($< 340\,\mathrm{km\,s^{-1}}$: Alatalo et al. 2011), which is indicative of an energetic phenomenon occurring in the galaxy. Actually, the presence of an AGN or LINER in the galaxy is implied by the radio, optical, and X-ray observations (Alatalo et al. 2011 and references therein). A powerful molecular wind from the nucleus of NGC 1266 is found, which is suggested to be driven by an AGN, since the estimated star-formation rate is insufficient to drive it. Our near-IR observation presents new evidence for the LINER nature of this galaxy.

NGC 2633 and NGC 2903 have consistent [Fe II]/Paβ and H_2/Brγ ratios with AGNs. The H- and K-band spectra of NGC 2633 were obtained by Vanzi, Alonso-Herrero, and Rieke (1998), who found that H_2 and Brγ were clearly detected, while [Fe II] 1.644 μm was not. The *EW*s of H_2 and Brγ measured by them, 3.0 ± 0.5 Å and 5.0 ± 0.5 Å, are in excellent agreement with our results. While Vanzi, Alonso-Herrero, and Rieke (1998) classified this galaxy as a starburst based on the optical [O I] 0.63 μm/Hα and near-IR [Fe II] 1.644 μm/Brγ line ratios, our new data indicate that NGC 2633 may be more like an AGN. In reality, NGC 2633 sits on the borderline of starbursts and AGNs in our diagram and on that of starbursts and "composite" objects in the classification diagram of Vanzi, Alonso-Herrero, and Rieke (1998), suggesting the contributions from both components. NGC 2903 is a well-known starburst galaxy, which has been studied at various wavelengths from radio to X-ray (e.g., Popping et al. 2010). While the majority of the radiation is thought to come from star-formation activity, Pérez-Ramírez et al. (2010) raise the possibility that a low-luminosity AGN is present in this galaxy based on its X-ray property. Our near-IR data support this possibility.

The [Fe II]/Paβ ratios of NGC 3034, Mrk 33, NGC 7625, and NGC 7714 are found to be at most 0.3, while no observation is available for the measurement of H_2 and Brγ. In the sample compiled by Rodríguez-Ardila, Riffel, and Pastoriza (2005), all sources with [Fe II]/Pa$\beta \leq 0.3$ have H_2/Br$\gamma \leq 0.3$. This may imply that the above four objects can most likely

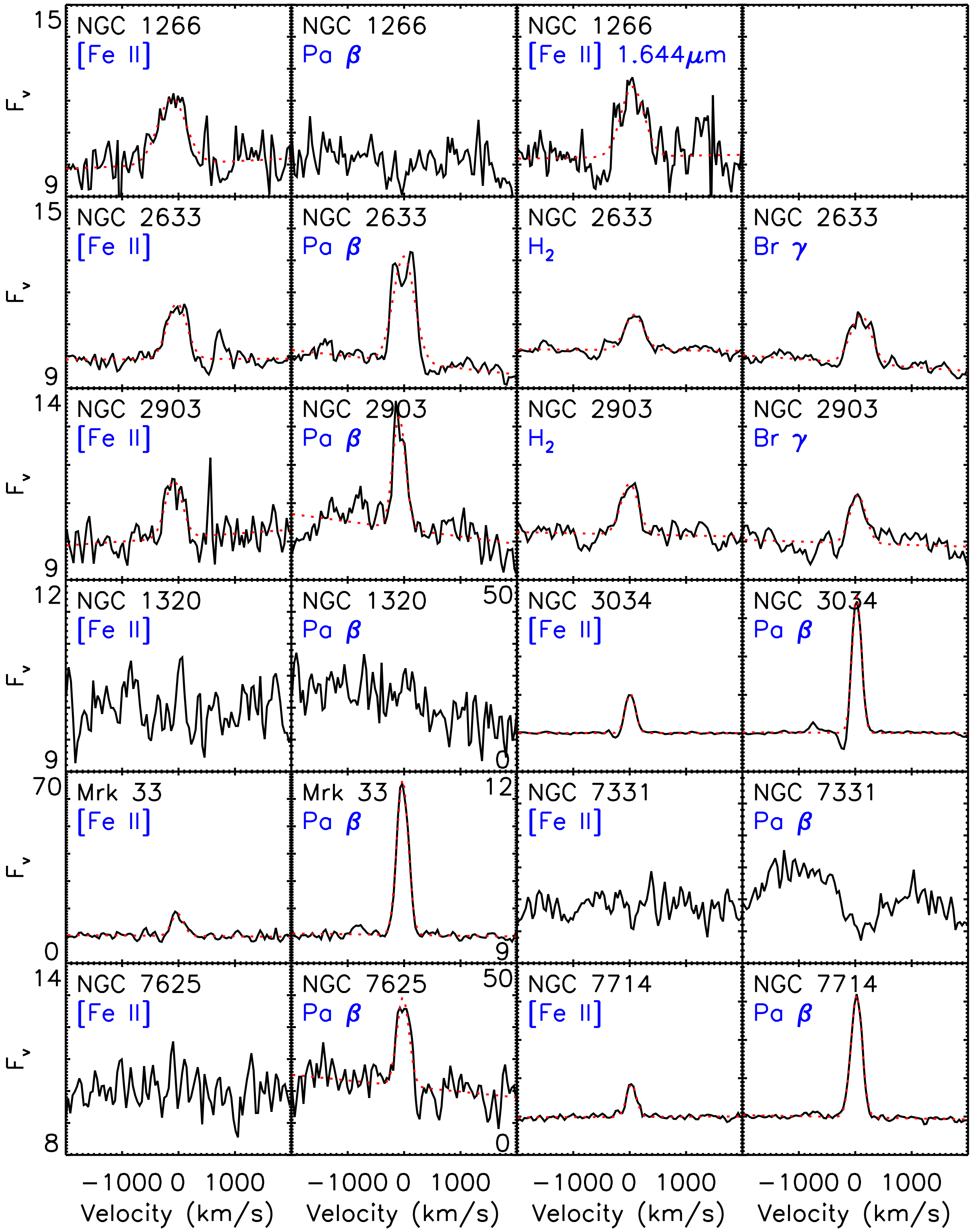

Fig. 1. ISLE spectra of the IRAS galaxies around [Fe II] 1.257 μm, Paβ (observed in J band), H_2 2.1213 μm, and Brγ (in K band) emission lines, as well as [Fe II] 1.644 μm (in H band) for NGC 1266. The wavelengths have been converted to the relative velocities to the line centers. The names of the targets and the emission lines are indicated at the top-left corner of each panel. The fitted Gaussian functions are also shown for the detected lines (red dotted lines). The fluxes are given per velocity in arbitrary scale, with consistent scaling for the same object.

Table 3. Measured emission-line properties.*

Object	[Fe II] 1.257 μm		Paβ		H_2 2.121 μm		Brγ	
	EW (Å)	*FWHM* (km s^{-1})	*EW* (Å)	*FWHM* (km s^{-1})	*EW* (Å)	*FWHM* (km s^{-1})	*EW* (Å)	*FWHM* (km s^{-1})
NGC 1266	5.3 ± 1.5	520 ± 60	<0.6	—	—	—	—	—
NGC 1320	<0.4	—	<0.3	—	—	—	—	—
NGC 2633	3.2 ± 0.5	320 ± 20	6.8 ± 0.5	360 ± 10	3.2 ± 0.5	260 ± 30	5.2 ± 0.5	310 ± 20
NGC 2903	2.3 ± 0.8	240 ± 40	3.4 ± 0.7	<300	3.6 ± 0.7	200 ± 30	3.2 ± 0.8	140 ± 40
NGC 3034	9.6 ± 0.4	<300	30.9 ± 1.3	<300	—	—	—	—
Mrk 33	9.3 ± 1.7	<300	59.7 ± 1.9	<300	—	—	—	—
NGC 7331	<0.2	—	<0.3	—	—	—	—	—
NGC 7625	<0.6	—	3.2 ± 0.7	<300	—	—	—	—
NGC 7714	8.1 ± 0.8	<300	34.5 ± 0.9	<300	—	—	—	—
Object	**[Fe II] 1.644 μm**							
	EW (Å)	*FWHM* (km s^{-1})						
NGC 1266	6.0 ± 1.5	450 ± 40						

* 2-σ upper limits are given for the fluxes of undetected emission lines.

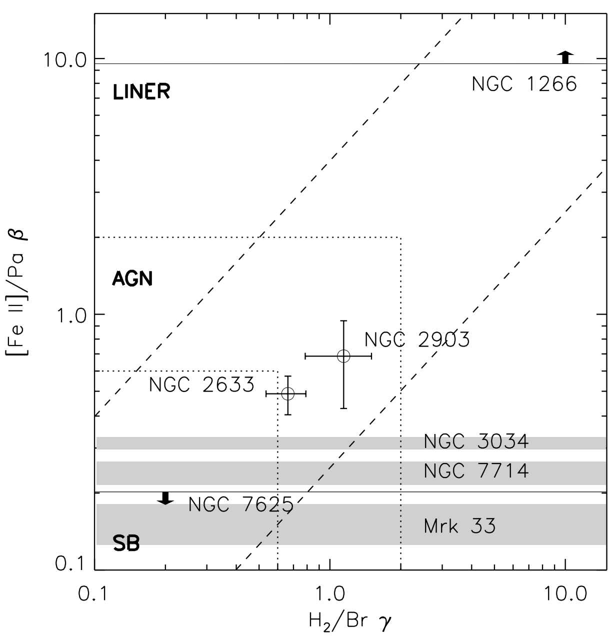

Fig. 2. Measured line-flux ratios of [Fe II]/Paβ and H_2/Brγ. The circles represent those objects with the four lines available, while the shaded area (1σ confidence level) or horizontal lines with arrows (the up and down arrows show the lower and upper limits, respectively) represent those without H_2 and Brγ measurements. The object names are indicated near the corresponding symbols. The dotted lines show the starburst(SB)/AGN/LINER demarcation proposed by Rodríguez-Ardila, Riffel, and Pastoriza (2005), while the dashed lines show the approximate envelope of object distribution in their compilation.

be categorized into starburst galaxies in figure 2, while additional observations of the H_2 and Brγ lines in these objects are needed for further discussion on this point. No clear evidence for the presence of AGNs has been obtained at other wavelengths, despite numerous observations dedicated to these well-known starburst galaxies. Another worth-noting point is the P Cygni profile observed in the [Fe II] and Paβ lines of NGC 3034 (see figure 1). The absorption features were detected at $\sim 250\,\mathrm{km\,s^{-1}}$ blueshift relative to the line centers, pointing to the presence of outflowing material in front of the line-emission region. These features are not found in the optical spectra of nuclear star clusters of this galaxy (e.g., Westmoquette et al. 2007; Konstantopoulos et al. 2009), which may be due to heavy dust obscuration. Observations with higher spatial resolution than the present one are required for locating this velocity component in the nuclear region of this galaxy.

4. Conclusion

In this paper we demonstrate the capability of the ISLE imager and spectrograph mounted on the OAO 1.88-m telescope to investigate near-IR line emissions of IRAS galaxies. The observation targets were selected from the IIFSCz based on the IRAS FSC. All of them are nearby galaxies at redshifts of $z < 0.01$. The [Fe II] 1.257 μm and Paβ emission lines were observed in a sample of nine galaxies, while the H_2 2.121 μm and Brγ lines were additionally observed for two of them. Based on the measured line-flux ratios, NGC 1266 is found to have a LINER, while NGC 2633 and NGC 2903 possibly harbor AGNs. On the other hand, no AGN signal was found for NGC 3034, Mrk 33, NGC 7625, and NGC 7714. In addition, we found the relatively large [Fe II] line widths of $\sim 500\,\mathrm{km\,s^{-1}}$ in NGC 1266 and the P Cygni profile of [Fe II] and Paβ lines in NGC 3034. The present work shows the potential ability of ISLE near-IR spectroscopy to shed new light on the nature of IR galaxies, either through a statistical survey of galaxies on diagnostic diagrams, such as figure 2, or an exploration of the spectral features found in individual galaxies.

This work was supported by Grant-in-Aid for Young Scientists (22684005) and the Global COE Program of Nagoya University “Quest for Fundamental Principles in the Universe” from JSPS and MEXT of Japan.

References

Alatalo, K., et al. 2011, ApJ, 735, 88
Farrah, D., et al. 2007, ApJ, 667, 149
Imanishi, M., Dudley, C. C., Maiolino, R., Maloney, P. R., Nakagawa, T., & Risaliti, G. 2007, ApJS, 171, 72
Konstantopoulos, I. S., Bastian, N., Smith, L. J., Westmoquette, M. S., Trancho, G., & Gallagher, J. S., III 2009, ApJ, 701, 1015
Larkin, J. E., Armus, L., Knop, R. A., Soifer, B. T., & Matthews, K. 1998, ApJS, 114, 59
Lonsdale, C. J., Farrah, D., & Smith, H. E. 2006, in Astrophysics Update 2, ed. J. W. Mason (Berlin: Springer-Verlag) 285
Matsuoka, Y., Kawara, K., & Oyabu, S. 2008, ApJ, 673, 62
Matsuoka, Y., Oyabu, S., Tsuzuki, Y., & Kawara, K. 2007, ApJ, 663, 781
Pérez-Ramírez, D., Caballero-García, M. D., Ebrero, J., & Leon, S. 2010, A&A, 522, A53
Pickles, A. J. 1998, PASP, 110, 863
Popping, G., Pérez, I., & Zurita, A. 2010, A&A, 521, A8
Ptak, A., Heckman, T., Levenson, N. A., Weaver, K., & Strickland, D. 2003, ApJ, 592, 782
Rodríguez-Ardila, A., Pastoriza, M. G., Viegas, S., Sigut, T. A. A., & Pradhan, A. K. 2004, A&A, 425, 457
Rodríguez-Ardila, A., Riffel, R., & Pastoriza, M. G. 2005, MNRAS, 364, 1041
Skrutskie, M. F., et al. 2006, AJ, 131, 1163
Soifer, B. T., Sanders, D. B., Madore, B. F., Neugebauer, G., Danielson, G. E., Elias, J. H., Lonsdale, C. J., & Rice, W. L. 1987, ApJ, 320, 238
Tran, Q. D., et al. 2001, ApJ, 552, 527
Vanzi, L., Alonso-Herrero, A., & Rieke, G. H. 1998, ApJ, 504, 93
Veilleux, S., Kim, D.-C., & Sanders, D. B. 2002, ApJS, 143, 315
Veilleux, S., Kim, D.-C., Sanders, D. B., Mazzarella, J. M., & Soifer, B. T. 1995, ApJS, 98, 171
Veilleux, S., Sanders, D. B., & Kim, D.-C. 1999, ApJ, 522, 139
Wang, L., & Rowan-Robinson, M. 2009, MNRAS, 398, 109
Westmoquette, M. S., Smith, L. J., Gallagher, J. S., III, O'Connell, R. W., Rosario, D. J., & de Grijs, R. 2007, ApJ, 671, 358
Yanagisawa, K., et al. 2006, Proc. SPIE, 6269, 62693
Yanagisawa, K., et al. 2008, Proc. SPIE, 7014, 701437